

# Sparticle masses from kinematic fitting at a muon collider <sup>1</sup>

Joseph D. Lykken\*

*\*Theoretical Physics Department  
Fermi National Accelerator Laboratory  
P.O. Box 500  
Batavia, IL 60510*

**Abstract.** Three case studies are presented of slepton pair production followed by two-body or quasi-two-body decays at a muon collider. Precision mass measurements are possible using a variety of kinematic fitting methods. Standard Model and supersymmetric backgrounds are easily controlled by kinematic cuts. In all three cases it appears that detector resolutions, not backgrounds or statistics, will dominate the final error bars. Polarized beams are not necessary to control SM backgrounds. However, without polarization it may be difficult in some cases to disentangle  $\tilde{l}_R$  from  $\tilde{l}_L$  signals.

## Introduction

A muon collider is in principle an excellent machine for precision studies of weak scale supersymmetry. Depending on  $\sqrt{s}$  and the SUSY mass spectrum, it may be possible to observe pair production of a half-dozen or more distinct sparticles. For R parity preserving SUSY, sparticle pair production is kinematically unconstrained, due to the pair of unmeasured LSP's. However in many cases each sparticle in the pair has a significant branching fraction for what is essentially a two-body decay:

$$\text{sparticle} \rightarrow \text{LSP} + \text{particle} \quad , \quad (1)$$

where "particle" refers to a fully reconstructible Standard Model particle ( $e$ ,  $\mu$ ,  $W$ ,  $Z$ , and possibly  $h_0$ ,  $t$ ), while the LSP is assumed to be the lightest neutralino  $\tilde{\chi}_1^0$ .

In these cases there are a variety of kinematic fitting methods for extracting sparticle masses. In this talk I will report on two such methods applied to smuon, selectron, and sneutrino production at a muon collider. Chargino production is not

---

<sup>1</sup>) Talk presented at the 4th International Conference on the Physics Potential and Development of  $\mu^+\mu^-$  Colliders, San Francisco, 10-12 December, 1997.

discussed, since for light fermionic sparticles the best method for a precision mass measurement is a threshold scan [1]. An interesting challenge for future investigation is the production of staus, stops, and the heavier chargino and neutralinos.

Sparticle production at a muon collider is similar in many respects to sparticle production at an  $e^+e^-$  machine. For the present analysis the most important differences are that the muon collider has (i) much higher energy reach, (ii) significantly lower advertised luminosity at comparable energies, (iii) little or no polarization available without taking a significant hit in luminosity, and (iv) large detector backgrounds from muon decays. These detector backgrounds are generally soft, but large fluctuations could cause problems for precision SUSY measurements. They will also impact on isolation cuts, determinations of missing  $E_T$ , and detector resolutions generally. These problems will be left to future study.

At a muon collider smuon pairs arise from both s and t channel production; the s channel production is through a virtual photon or Z, while the t channel diagram involves the exchange of a neutralino. The s and t channel contributions interfere destructively, but this effect will not be important for the examples considered here, where the t channel production is dominant. Selectron production proceeds only through the s channel, and is thus suppressed in the examples. Muon sneutrino production proceeds only through the t channel, and is thus competitive with smuons.

In both supergravity (sugra) and gauge mediated models, the  $\tilde{l}_R$ 's are lighter than the  $\tilde{l}_L$ 's. Independent of the SUSY model,  $\tilde{l}_R$ 's decay almost 100% via a single two-body mode:

$$\tilde{\mu}_R \rightarrow \tilde{\chi}_1^0 \mu \quad ; \quad \tilde{e}_R \rightarrow \tilde{\chi}_1^0 e \quad . \quad (2)$$

The branching fractions of the  $\tilde{l}_L$ 's and  $\tilde{\nu}_L$ 's are model dependent. The important decay modes for, e.g.,  $\tilde{\mu}_L$  are:

$$\begin{aligned} \tilde{\mu}_L \rightarrow & \quad \tilde{\chi}_1^0 \mu \\ & \quad \tilde{\chi}_2^0 \mu \\ & \quad \tilde{\chi}_1^\pm \nu_\mu \quad . \end{aligned} \quad (3)$$

## Kinematics

The basic kinematics can be understood by considering pair production of  $\tilde{\mu}_R$ :

$$\begin{aligned} \mu^+ \mu^- \rightarrow & \quad \tilde{\mu}_R(p_1) \tilde{\mu}_R(p_2) \\ & \quad \tilde{\mu}_R(p_1) \rightarrow \quad \tilde{\chi}_1^0(p_3) \mu(p_4) \\ & \quad \tilde{\mu}_R(p_2) \rightarrow \quad \tilde{\chi}_1^0(p_5) \mu(p_6) \quad . \end{aligned} \quad (4)$$

Each event consists of an acoplanar dimuon pair plus missing  $E_T$ . Six measurements are made, i.e., the 3-momenta of the two muons. The event is characterized by 13

**TABLE 1.** Sparticle and Higgs spectrum for LHC Point 5, which corresponds to minimal sugra parameters  $m_0=100$  GeV,  $m_{1/2}=300$  GeV,  $A_0=0$ ,  $\tan\beta=2.1$ , and  $\text{sgn}(\mu)=1$ .

Particle	Mass (GeV)	Particle	Mass (GeV)
$\tilde{\chi}_1^0$	119	$\tilde{\chi}_2^0$	228
$\tilde{\chi}_1^\pm$	228	$\tilde{\chi}_2^\pm$	565
$\tilde{e}_R$	157	$\tilde{e}_L$	241
$\tilde{\mu}_R$	157	$\tilde{\mu}_L$	241
$\tilde{\nu}_L$	232	$\tilde{g}$	754
$\tilde{t}_1$	448	$\tilde{b}_1$	604
$h_0$	94	$H_A$	657

kinematic variables: the four 3-momenta of the final state plus the common LSP mass. There are 5 kinematic constraints: one from the assumption that the two smuons have the same mass, and the rest from the known initial state 4-momentum. This leaves 2 undetermined variables in the event, which we may take as  $M_{\tilde{\mu}}$ ,  $M_{\text{LSP}}$ .

The kinematic endpoint method arises from the following expression for the energy of each muon as measured in the rest frame of its parent smuon:

$$E_\mu^0 = \frac{M_{\tilde{\mu}}^2 - M_{\text{LSP}}^2}{2M_{\tilde{\mu}}} \quad , \quad (5)$$

where we are neglecting the muon mass. The maximum and minimum boosts from this frame to the lab frame then provides us with two kinematic endpoints  $E_\mu^{\text{max}}$ ,  $E_\mu^{\text{min}}$ , in the muon energy spectrum. A precision measurement of both endpoints allows us to extract both  $M_{\tilde{\mu}}$  and  $M_{\text{LSP}}$ . Note that this method requires good statistics to be useful, and does not take advantage of all the kinematic information in the event.

Another kinematic method, developed by Feng and Finnell for  $e^+e^-$  studies, extracts  $M_{\tilde{\mu}}$  assuming a precision value of  $M_{\text{LSP}}$  is already known from other sources and thus can be used as an input. This method starts with the relation

$$M_{\tilde{\mu}}^2 = \frac{1}{4}s - |\vec{p}_3|^2 - |\vec{p}_4|^2 - 2|\vec{p}_3||\vec{p}_4|\cos\theta_{34} \quad . \quad (6)$$

For given input value of  $M_{\text{LSP}}$ , the only unknown on the right hand side is  $\theta_{34}$ , the angle between the 3-vectors  $\vec{p}_3$  and  $\vec{p}_4$ . This angle is then estimated, event by event, by a certain function of measured variables. This function has the property that the error of the estimate goes to zero in the limit that the two LSP's are back-to-back in the lab frame. For  $\sqrt{s}/2 \gg M_{\tilde{\mu}} \gg M_{\text{LSP}}$ , the mass estimates peak strongly around the true value, and precise results are possible even for rather sparse data.

A third kinematic method, which is currently under investigation, involves adapting the likelihood methods developed for extracting the top quark mass from the dilepton channel. This method is also well-suited to sparser data sets.

## Simulations

Simulations were performed using PYTHIA v6.1 [3] coupled to the ATLFAST v1.25 [4] fast detector simulator. Note that the small differences in the sparticle spectra produced by PYTHIA and ISAJET [5] make a difference for the analysis done here. The ATLFAST defaults were used for lepton isolation and jet reconstruction. Smearing was not included, and no attempt was made to include detector backgrounds. Thus “precision” here refers only to statistics and to SUSY signal versus Standard Model (SM) backgrounds and SUSY backgrounds.

### Sleptons at LHC point 5

This first study overlaps with the analysis presented by Frank Paige at the Fermilab workshop [6]. LHC point 5 is a minimal supergravity reference point described in Table 1. For dimuon and dielectron production at  $\sqrt{s}=600$  GeV, cuts were imposed similar to those of [6]:

- Exactly two isolated e or  $\mu$  leptons and no jets,
- $E > 10$  GeV and  $|\eta| < 1.3$  for each lepton,

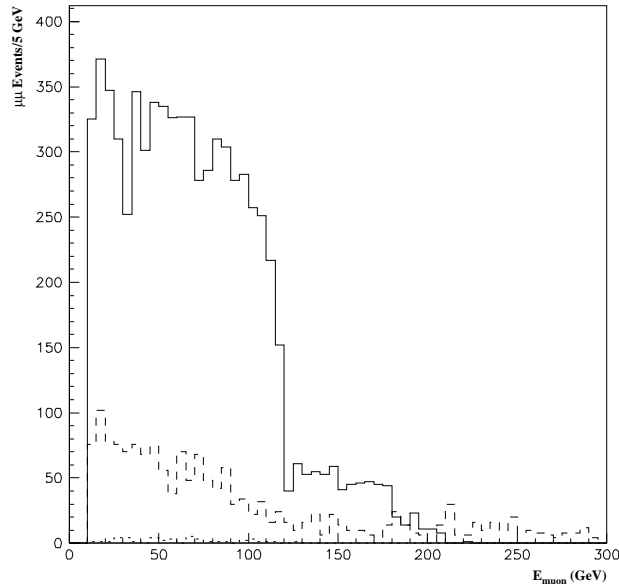


**FIGURE 1.** Dimuon production after cuts,  $20 \text{ fb}^{-1}$  at  $\sqrt{s}=600$  GeV for LHC point 5. The solid line is the total smuon signal. The dashed line is the sum of the Standard Model backgrounds; the dotted line is the background from chargino pairs.

- $\Delta\phi_{1,2} < 0.9\pi$ ,
- $|\vec{p}_{T,1} + \vec{p}_{T,2}| > 10 \text{ GeV}$ , and
- missing  $E_T > 20 \text{ GeV}$ .

Note that missing  $E_T$  signatures are degraded at a muon collider detector, due to the 20 degree forward and backward dead cones needed for shielding. This is not a crucial point for the present analysis, however.

The signal acceptance with these cuts is approximately 40%. The cuts are very efficient at eliminating backgrounds. The simulations included the six most important SM backgrounds; these are:

- $W^+W^-$  pair production,
- $\gamma\mu \rightarrow W\nu_\mu$ ,
- Drell-Yan,
- $\gamma\mu \rightarrow Z\mu$ ,
- $\gamma\gamma \rightarrow l^+l^-$ , and
- $ZZ$  pairs.

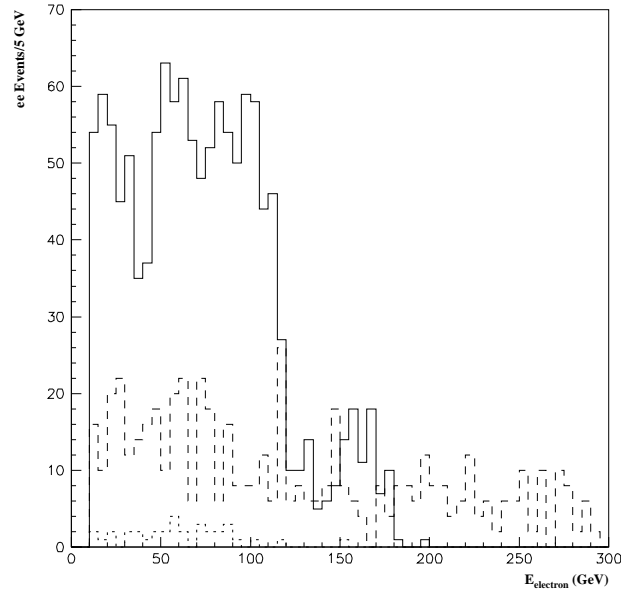


**FIGURE 2.** Dielectron production after cuts,  $20 \text{ fb}^{-1}$  at  $\sqrt{s}=600 \text{ GeV}$  for LHC point 5. The solid line is the total selection signal. The dashed line is the sum of the Standard Model backgrounds; the dotted line is the background from chargino pairs.

The main SUSY background is from chargino pair production, with both charginos decaying leptonically.

Figures 1 and 2 show the dimuon and dielectron event rates plotted versus muon or electron energy, with 5 GeV bins. The SM backgrounds after cuts are rather flat and encouraging small, even for the dielectron case. The SUSY background is negligible. For  $20\text{fb}^{-1}$  of integrated luminosity, Figure 2 also reflects the rather poor statistics of selectron production. This is not surprising given that the total cross section is only 64 fb. The situation is noticeably better for smuon production, where the cross section is 400 fb.

Figure 3 shows the  $\mu\mu$ - $ee$  flavor subtracted slepton signal, after cuts, broken down into the its three components: RR, RL+LR, and LL. The integrated luminosity is  $100\text{fb}^{-1}$  to enhance the statistics. As discussed in [6], this figure shows a rather complicated structure, reflecting the fact that there are eight distinct kinematic endpoints affecting the distribution. These are:

$$\begin{aligned}
 \tilde{l}_R\tilde{l}_R &: & 118\text{ GeV}, & & 9\text{ GeV}; \\
 \tilde{l}_R\tilde{l}_L &: & 105\text{ GeV}, & & 11\text{ GeV}; \\
 \tilde{l}_L\tilde{l}_R &: & 208\text{ GeV}, & & 40\text{ GeV}; \\
 \tilde{l}_L\tilde{l}_L &: & 181\text{ GeV}, & & 46\text{ GeV}.
 \end{aligned}
 \tag{7}$$

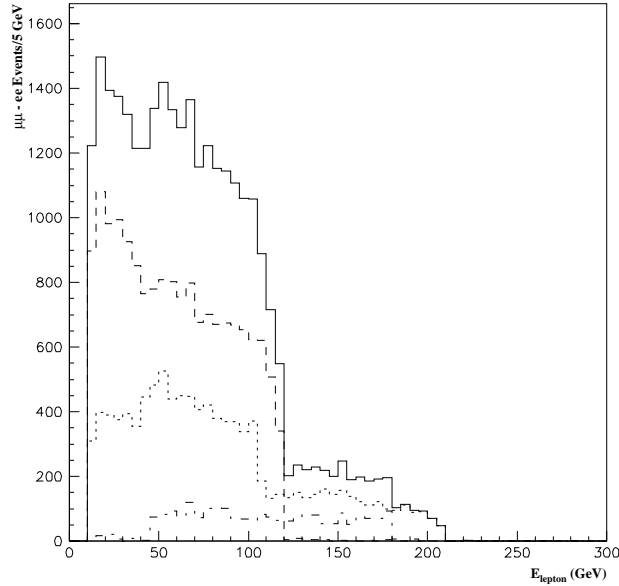


**FIGURE 3.** Flavor subtracted slepton signal,  $100\text{fb}^{-1}$  at  $\sqrt{s}=600\text{ GeV}$  for LHC point 5. The solid line is the total smuon + selectron signal. The dashed, dotted, and dot-dashed lines are from  $\tilde{l}_R\tilde{l}_R$ ,  $\tilde{l}_R\tilde{l}_L+\tilde{l}_L\tilde{l}_R$ , and  $\tilde{l}_L\tilde{l}_L$ , respectively.

Comparing with Figures 1,2, it appears that with  $20 \text{ fb}^{-1}$  and a perfect detector, one can determine the endpoints at 118, 208, and 181 GeV to an accuracy of one bin or better. The other endpoints look very challenging.

The situation improves if we include the Feng-Finnell estimate for the smuon mass. This is shown in Figure 4, plotted with 1 GeV bins. The SM background shown is completely negligible. Because of the strong peaking, which actually resembles a sharp edge, it is trivial to extract the  $\tilde{\mu}_R$  mass with an accuracy of one bin or better. This assumes that the  $\tilde{\chi}_1^0$  mass is already known to within 1 GeV. Similar results are obtained for the  $\tilde{e}_R$ , with somewhat worse statistics.

## Heavy sleptons

The second study is for the heavy sugra point described in Table 2. The results are for dimuon and dielectron production at  $\sqrt{s} = 1400 \text{ GeV}$ , using the same cuts as in the previous example.

Figure 5 shows the flavor subtracted slepton signal corresponding to  $1000 \text{ fb}^{-1}$  of integrated luminosity. Comparing with Figure 3, one notes several differences. In the present case the signal is completely dominated by RR production. This is because the branching fraction for  $\tilde{\mu}_L$  or  $\tilde{e}_L$  decay to muon or electron plus  $\tilde{\chi}_1^0$  is

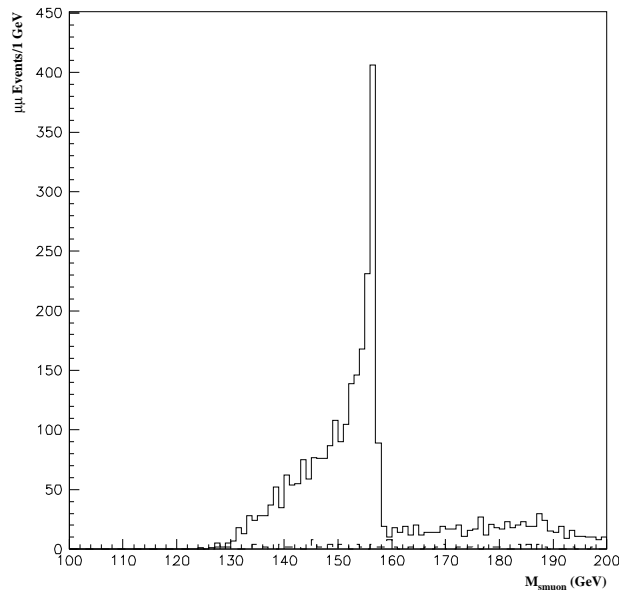


**FIGURE 4.** Dimuon production after cuts,  $20 \text{ fb}^{-1}$  at  $\sqrt{s}=600 \text{ GeV}$  for LHC point 5. The solid line is the total smuon signal, plotted versus the Feng-Finnell estimate for the smuon mass. The dashed line is the sum of the Standard Model backgrounds.

**TABLE 2.** Sparticle and Higgs spectrum for the heavy sugra point, which corresponds to minimal sugra parameters  $m_0=500$  GeV,  $m_{1/2}=350$  GeV,  $A_0=0$ ,  $\tan\beta=2$ , and  $\text{sgn}(\mu)=-1$ .

Particle	Mass (GeV)	Particle	Mass (GeV)
$\tilde{\chi}_1^0$	145	$\tilde{\chi}_2^0$	290
$\tilde{\chi}_1^\pm$	290	$\tilde{\chi}_2^\pm$	809
$\tilde{e}_R$	519	$\tilde{e}_L$	561
$\tilde{\mu}_R$	519	$\tilde{\mu}_L$	561
$\tilde{\nu}_L$	558	$\tilde{g}$	886
$\tilde{t}_1$	597	$\tilde{b}_1$	763
$h_0$	84	$H_A$	1083

only 16%. At this heavy sugra point, the  $\tilde{\mu}_L$  decays predominantly to either  $\tilde{\chi}_1^\pm \nu_\mu$  or  $\tilde{\chi}_2^0 \mu$ . Subsequent decays in these modes are unlikely to pass the cuts.

Since RR production now dominates, there are effectively only two kinematic endpoints: 539 GeV and 106 GeV. Note that the lower endpoint is now sufficiently large not to be distorted or hidden by the cuts. Both edges are very sharp in Figure 5. The SM backgrounds after cuts are negligible. Thus with a perfect detector one could extract the masses of both  $\tilde{\mu}_R$  and  $\tilde{\chi}_1^0$  with an accuracy better than 5 GeV.

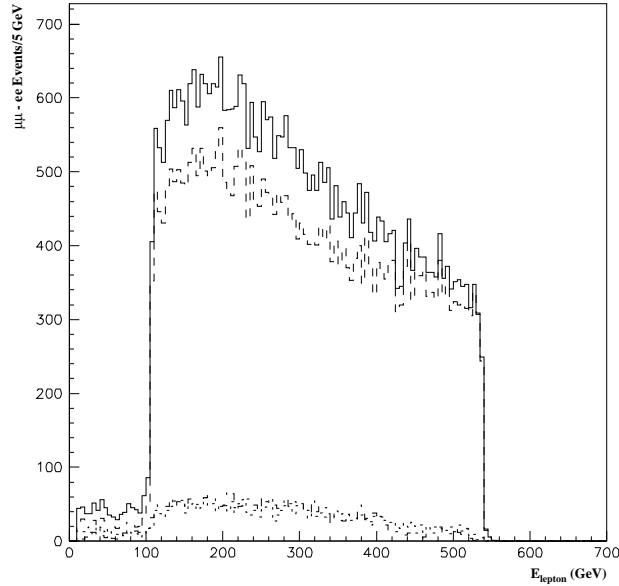


**FIGURE 5.** Flavor subtracted slepton signal,  $1000 \text{ fb}^{-1}$  at  $\sqrt{s}=1400$  GeV for the heavy sugra point. The solid line is the total smuon + selectron signal. The dashed, dotted, and dot-dashed lines are from  $\tilde{l}_R \tilde{l}_R$ ,  $\tilde{l}_R \tilde{l}_L + \tilde{l}_L \tilde{l}_R$ , and  $\tilde{l}_L \tilde{l}_L$ , respectively.

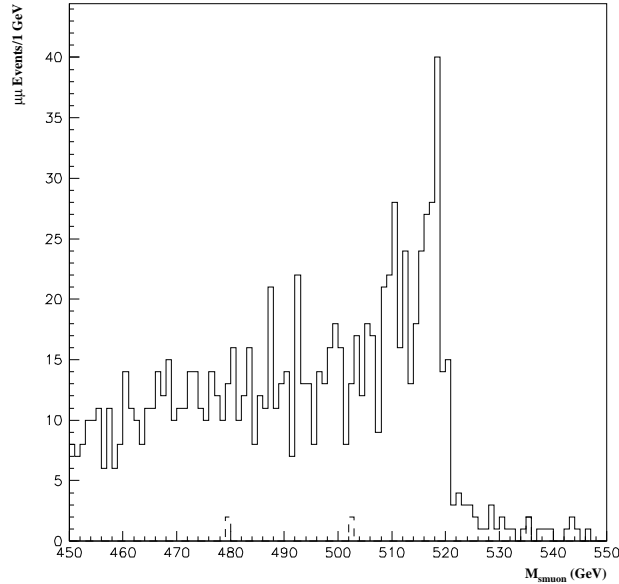


Figure 6 shows the Feng-Finnell plot for the heavy sugra point. The SM backgrounds shown are negligible. Again we see strong edgelike peaking around the actual  $\tilde{\mu}_R$  mass of 519 GeV. It is clearly possible to extract the mass with an accuracy of one bin or better. This assumes that the  $\tilde{\chi}_1^0$  mass is already known to within 1 GeV. Similar results are obtained for the  $\tilde{e}_R$ , but with poor statistics.

## Sneutrino pair production

Muon sneutrino pair production fits our kinematic scenario, provided that the sneutrino has a substantial branching fraction to  $\tilde{\chi}_1^\pm \mu$ . The chargino will decay predominantly to  $\tilde{\chi}_1^0$  plus jets. Thus the signature is an acoplanar dimuon pair plus missing  $E_T$  plus jets. Note that, in the presence of the R parity violating coupling LLE, s-channel resonant production of single sneutrinos may also be possible at a muon collider [7].

Here we have studied the sugra point described in Table 3, for production at  $\sqrt{s} = 800$  GeV. The branching fraction for the muon  $\tilde{\nu}_L$  into  $\tilde{\chi}_1^\pm \mu$  is 56%, while the branching fraction for  $\tilde{\chi}_1^\pm$  into  $\tilde{\chi}_1^0$  plus jets is 65%. We will employ the same cuts as previously, except that we now require two or more reconstructed jets (cone radius  $R = 0.4$ ).



**FIGURE 6.** Dimuon production after cuts,  $100 \text{ fb}^{-1}$  at  $\sqrt{s}=1400$  GeV for the heavy sugra point. The solid line is the total smuon signal, plotted versus the Feng-Finnell estimate for the smuon mass. The dashed line is the sum of the Standard Model backgrounds.

**TABLE 3.** Sparticle and Higgs spectrum for the third sugra point, which corresponds to minimal sugra parameters  $m_0=225$  GeV,  $m_{1/2}=200$  GeV,  $A_0=0$ ,  $\tan\beta=2$ , and  $\text{sgn}(\mu)=1$ .

Particle	Mass (GeV)	Particle	Mass (GeV)
$\tilde{\chi}_1^0$	77	$\tilde{\chi}_2^0$	146
$\tilde{\chi}_1^\pm$	144	$\tilde{\chi}_2^\pm$	449
$\tilde{e}_R$	240	$\tilde{e}_L$	270
$\tilde{\mu}_R$	240	$\tilde{\mu}_L$	270
$\tilde{\nu}_L$	262	$\tilde{g}$	536
$\tilde{t}_1$	310	$\tilde{b}_1$	450
$h_0$	88	$H_A$	560

Figure 7 shows the Feng-Finnell mass estimate after cuts plotted in 1 GeV bins. Shown is the total signal from all SUSY production mechanisms. The SM background after cuts is negligible. The signal acceptance for muon sneutrino pairs after cuts is about 4%. Thus, despite a rather large cross section (over 500 fb) the plot has rather poor statistics. Nevertheless we again see strong edgelike peaking at the true  $\tilde{\nu}_L$  mass of 262 GeV.

It is interesting to note that a previous study of sneutrino pair production at

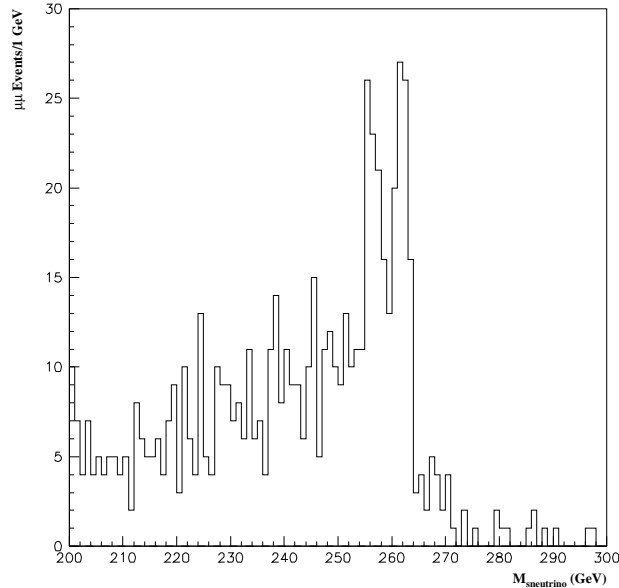


**FIGURE 7.** Dimuons plus two or more jets, after cuts,  $20 \text{ fb}^{-1}$  at  $\sqrt{s}=800$  GeV for the second sugra point. Shown is the total SUSY signal, plotted versus the Feng-Finnell estimate for the sneutrino mass.

$e^+e^-$  colliders [8] relied on the trilepton plus missing  $E_T$  plus jets channel to kill SM backgrounds. For our study point this does not appear to be necessary. Furthermore, our complementary dilepton channel has five times the rate, before cuts, as the trilepton channel.

## Conclusions

A variety of precision sparticle mass measurements are possible at a muon collider using kinematic methods such as those discussed here. Polarized beams are not necessary to control SM backgrounds. However, without polarization it may be difficult in some cases to disentangle  $\tilde{l}_R$  from  $\tilde{l}_L$  signals.

It seems likely that in most cases detector resolutions, not backgrounds or statistics, will dominate the final error bars. Thus it will be crucial to perform simulations with a realistic mock-up of a muon collider detector.

Adequate statistics for the type of analysis presented here correspond to integrated luminosities of at least  $20 \text{ fb}^{-1}$  for  $\sqrt{s}$  in the range 500 to 800 GeV. For heavy sparticles and  $\sqrt{s} \gtrsim 1 \text{ TeV}$ , the minimum useful integrated luminosity is about  $100 \text{ fb}^{-1}$ .

This research was supported by the Fermi National Accelerator Laboratory, which is operated by Universities Research Association, Inc., under contract no. DOE-AC02-76CHO3000.

## REFERENCES

1. Berger, M.S., these proceedings; hep-ph/9802213.
2. Feng, J., and Finnell, D., *Physical Review* **D49** 2369 (1994).
3. Sjostrand, T., *Computer Phys. Commun.* **82** 74 (1994).
4. Richter-Was, E., Froidevaux, D., and Poggioli, L., ATLAS internal note PHYS-NO-079, 1996.
5. Baer, H., Paige, F., Protopopescu, S., and Tata, X., in *Physics at Current Accelerators and Supercolliders*, ed. Hewett, J., White, A., and Zeppenfeld, D., Argonne National Lab, 1993.
6. Paige, F., proceedings of *Workshop on Physics at the First Muon Collider and at the Front End of a Muon Collider*, Fermilab, 6-9 Nov. 1997; hep-ph/9801396.
7. Feng, J., these proceedings; hep-ph/9801248.
8. Baer, H., Munroe, R., and Tata, X., *Physical Review* **D54** 6735 (1996).